EFFICIENT ANALYSIS OF MEDICAL IMAGE DE-NOISING FOR MRI AND ULTRASOUND IMAGES

MOHAMED SALEH ABUAZOUM

A dissertation submitted in fulfillment of the requirement for the award of the Degree Master of Electrical Engineering

Faculty of Electrical and Electronic Engineering
Universiti Tun Hussein Onn Malaysia

January 2012

ABSTRACT

Magnetic resonance imaging (MRI) and ultrasound images have been widely exploited for more truthful pathological changes as well as diagnosis. However, they suffer from a number of shortcomings and these includes: acquisition noise from the equipment, ambient noise from the environment, the presence of background tissue, other organs and anatomical influences such as body fat, and breathing motion. Therefore, noise reduction is very important, as various types of noise generated limits the effectiveness of medical image diagnosis. In this study, an efficient analysis of MRI and ultrasound modalities is performed. Three experiments have been carried out that include various filters (Median, Gaussian and Wiener filter) and evaluating the outcomes of medical image de-noising after applying these three filters by calculating the peak signal-to-noise ratio (PSNR), which shows that Gaussian filter is better than Median and Wiener filter.

TABLE OF CONTENTS

CHAPTER	TITLE	PAGE
	DISSERTATION STATUS CONFIRMATION	
	SUPERVISOR'S DECLARATION	
	TITLE PAGE	i
	DECLARATION	ii
	DEDICATION	iii
	ACKNOWLEDGEMENT	iv
	ABSTRACT	v
	TABLE OF CONTENTS	vi
	LIST OF TABLES	x
	LIST OF FIGURES	xi
I	**INTRODUCTION**	1
	1.1 Background	1
	1.2 Problem Statements	2
	1.3 Objectives	3
	1.4 Scopes	3

CHAPTER	TITLE	PAGE
II	**LITERATURE REVIEW**	4
	2.1 Related Works	4
	2.1.1 Ultrasound de-noising	4
	2.1.2 MRI de-noising	5
	2.2 Medical imaging	6
	2.3 Comparison between MRI and ultrasound imaging	8
	2.4 Image noise	9
	2.4.1 Amplifier Noise (Gaussian Noise)	9
	2.4.2 Salt-and-pepper Noise	10
	2.4.3 Speckle Noise	10
	2.5 Classification of de-noising filters	11
	2.6 De-noising filters review	12
	2.6.1 Median filter	12
	2.6.2 Gaussian filter	12
	2.6.3 Wiener filter	13
	2.7 Peak signal-to-noise ratio (PSNR)	15
III	**METHODOLOGY**	17
	3.1 The concept of de-noising filters	17
	3.1.1 Convolution	18
	3.1.2 How does Median filter work?	19
	3.1.3 How does Gaussian filter work?	21
	3.1.4 How does Wiener filter work?	25
	3.2 PSNR Calculation	29
	3.3 Description of Methodology	30
	3.4 Median filter implementation	31
	3.4.1 Applying Median filter on MRI image	31
	3.4.2 Applying Median filter on Ultrasound Image	32

3.5 Gaussian filter implementation 34

3.4.3 Applying Gaussian filter on MRI image 34

3.4.4 Applying Gaussian filter on Ultrasound Image 35

3.6 Wiener filter implementation 36

3.6.1 Applying Wiener filter on MRI image 36

3.6.2 Applying Wiener filter on Ultrasound Image 38

IV RESULTS AND ANALYSIS 40

4.1 Result of Median filter on MRI and ultrasound 40

4.2 Result of Gaussian filter on MRI and ultrasound 42

4.3 Result of Wiener filter on MRI and ultrasound 44

V CONCLUSION AND RECOMMENDATION 49

5.1 Conclusion 49

5.2 Recommendation 50

REFERENCES 51

LIST OF FIGURES

FIGURE NO.	TITLE	PAGE
2.1	Classification of de-noising filters	11
3.1	(a) Pixels of image (b) Kernel of filter	18
3.2	Sorting neighbourhood values and determine median value	19
3.3	Assumed pixels window represented on MRI image	20
3.4	Movement of the window 3×3 (mask) on the pixels	20
3.5	Sorting the pixels and determining middle pixel value	20
3.6	Pixels window after applying Median filter on all pixels	21
3.7	One dimensional Gaussians	21
3.8	Two dimensional Gaussians	22
3.9	3×3 windows with $\boldsymbol{\sigma} = 0.849$, $\boldsymbol{\sigma} = 1$, $\boldsymbol{\sigma} = 2$	23
3.10	3×3 windows with $\sigma = 0.849$	23
3.11	Assumed pixels window represented on MRI image	23
3.12	Movement of the window 3 x 3 (mask) on the pixels	24
3.13	3×3 windows with $\sigma = 0.849$, first window of MRI pixels	24
3.14	Pixels window after applying Gaussian filter on all pixels	25
3.15	Assumed pixels window represented on MRI image	26
3.16	Movement of the window 3 x 3 (mask) on the pixels	26
3.17	First window of the pixels	26
3.18	Pixels window after applying Wiener filter on all pixels	29
3.19	Image de-noising chart	30
3.20	(a) MRI image (b) Ultrasound image	31

FIGURE NO.	TITLE	PAGE
3.21	MRI image	31
3.22	Noisy MRI image	32
3.23	Ultrasound image	33
3.24	Noisy ultrasound image	33
3.25	MRI image	34
3.26	Noisy MRI image	34
3.27	Ultrasound image	35
3.28	Noisy ultrasound image	36
3.29	MRI image	37
3.30	Noisy MRI image	37
3.31	Ultrasound image	38
3.32	Noisy ultrasound image	38
4.1	PSNR results of de-noised MRI image by Median filter with windows size from (1×1) to (6×6) with best PSNR= 14.01 dB	40
4.2	De-noised MRI image by Median filter	41
4.3	PSNR results of de-noised ultrasound image by Median filter with windows size from (1×1) to (6×6) with best PSNR= 14.98 dB	41
4.4	De-noised ultrasound image by Median filter	42
4.5	PSNR results of de-noised MRI image by Gaussian filter with windows size from (1×1) to (6×6), $\sigma = 0.849$, with best PSNR= 15.53 dB	42
4.6	De-noised MRI image by Gaussian filter	43
4.7	PSNR results of de-noised Ultrasound Image by Gaussian filter with windows size from (1×1) to (6×6), $\sigma = 0.849$, with best PSNR= 17.37 dB	43
4.8	De-noised ultrasound image by Gaussian filter	44
4.9	PSNR results of de-noised MRI image by Wiener filter with windows size from (1×1) to (6×6), with best PSNR= 15.35 dB	44

FIGURE NO.	TITLE	PAGE
4.10	De-noised MRI image by Wiener filter	45
4.11	PSNR results of de-noised Ultrasound Image by Wiener filte with windows size from (1×1) to (6×6), with best PSNR= 17.27 dB	45
4.12	De-noised ultrasound image by Wiener filter	46
4.13	(a1) Original MRI, (a2) Original ultrasound image, (b1) Noisy MRI by White Gaussian Noise, (b2) Noisy ultrasound image by White Gaussian Noise, (c1) De-noised MRI by Median filter, (c2) De-noised ultrasound image by Median filter, (d1) De-noised MRI by Gaussian filter, (d2) De-noised ultrasound image by Gaussian filter, (e1) De-noised MRI by Wiener filter, (e2) De-noised ultrasound image by Wiener filter.	47

LIST OF TABLES

TABLE NO.	TITLE	PAGE
2.1	Summary of previous study	6
2.2	Comparison between MRI and ultrasound image	8
4.1	PSNR results of applying Median, Wiener and Gaussian filter on three ultrasound images (US1, US2 and US3) and three MRI images (MRI1, MRI2 and MRI3)	46

CHAPTER I

INTRODUCTION

1.1 Background

The influence and impact of digital images on modern society is tremendous, and image processing is now a critical component in science and technology. The rapid progress in computerized medical image reconstruction, and the associated developments in analysis methods and computer-aided diagnosis, has propelled medical imaging into one of the most important sub-fields in scientific imaging [1].

The arrival of digital medical imaging technologies such as positron emission tomography (PET), magnetic resonance imaging (MRI), computerized tomography (CT) and ultrasound Imaging has revolutionized modern medicine [2]. Today, many patients no longer need to go through invasive and often dangerous procedures to diagnose a wide variety of illnesses. With the widespread use of digital imaging in medicine today, the quality of digital medical images becomes an important issue. To achieve the best possible diagnosis it is important that medical images be sharp, clear, and free of noise and artifacts. While the technologies for acquiring digital medical images continue to improve, resulting in images of higher and higher resolution and quality, removing noise in these digital images remains one of the major challenges in the study of medical imaging, because they could mask and blur important subtle features in the images, many proposed de-noising techniques have their own problems. Image de-noising still remains a challenge for researchers because noise removal introduces artifacts and causes blurring of the images [3].

This project describes different methodologies for noise reduction (or de-noising) giving an insight as to which algorithm should be used to find the most reliable estimate of the original image data given its degraded version. Noise modelling in medical images is greatly affected by capturing instruments, data transmission media, image quantization and discrete sources of radiation. Different algorithms are used depending on the noise model. Most of images are assumed to have additive random noise which is modelled as a white Gaussian noise. Therefore it is required to exterminate a variety of types of de-noising algorithm for MRI and ultrasound modalities.

1.2 Problem Statements

Medical images such as magnetic resonance imaging (MRI) and ultrasound images have been widely exploited for more truthful pathological changes as well as diagnosis. However, they suffer from a number of shortcomings and these includes: acquisition noise from the equipment, ambient noise from the environment, the presence of background tissue, other organs and anatomical influences such as body fat, and breathing motion. Therefore, noise reduction is very important, as various types of noise generated limits the effectiveness of medical image diagnosis. The amount of the noise has the tendency of being either relatively high or low. Thus, it could harshly degrade the image quality and cause some loss of image information details.

1.3 Objectives

The major objective of this project is noise reduction for measurable objectives are as follows:

1. To investigate medical Image for better diagnosis.
2. To implement the different types of de-noising filters.
3. To observe the images after the de-noising.
4. To evaluate the best from de-noising filters.

1.4 Scopes

This project is primarily concerned with The scope of the project is to focus on noise removal techniques for medical images (MRI) and Ultrasound:

1. Using Matlab Simulink software for modalities analysis.
2. Using Image Processing Toolbox to adding noise and to apply de-noising algorithms.
3. Using some of de-noising filters with different coefficients and comparing between the results.

CHAPTER II

LITERATURE REVIEW

2.1 Related Works

2.1.1 Ultrasound de-noising

Some of the best known standard de-speckling filters are the methods of Lee ,Frost and Kuan filter [4], [5]. These filters use the second-order sample statistics within a minimum mean squared error estimation approach. Another common de-speckling approach is the homomorphic Wiener filter [6], where the image is first subjected to a logarithmic transform and then filtered with an adaptive filter for additive Gaussian noise [7]. Lee filter is based on the approach that if the variance over an area is low, then the smoothing will be performed. Otherwise, if the variance is high (e.g. near edges), smoothing will not be performed. Kuan filter [4] is considered to be more superior to the Lee filter. It does not make approximation on the noise variance within the filter window. The filter simply models the multiplicative model of speckle into an additive linear form, but it relies on the equivalent numbers of looks (ENL) from an image to determine a different weighted W to perform the filtering as shown in Eq (1).

$$W = \left(1 - \frac{Cu}{Ci}\right)(1 + Cu) \tag{1}$$

Where Cu is the noise variation coefficient and Ci is the image variation coefficient. Next, the Wiener is a low pass filter that filters an intensity image that has been degraded by constant power additive noise. It uses a pixel wise adaptive Wiener method based on statistics estimated from a local neighbourhood of each pixel.

2.1.2 MRI de-noising

A multitude of variation methods based on partial differential equations have been developed for a wide variety of images and applications [8], with some of these have been applied to MRI [9], [10]. However, such methods impose certain kinds of models on local image structure that are often too simple to capture the complexity of anatomical MR images. These methods, typically, does not considered the bias introduced by Rician noise.

Healy and Weaver [11] were among the first to apply soft-thresholding based on wavelet techniques for de-noising MR images. Nowak [12], operating on the square magnitude MRI image, includes a Rician noise model in the threshold-based wavelet de-noising scheme and thereby corrects for the bias introduced by the noise. Pizurica et al. [13] rely on the prior knowledge of the correlation of wavelet coefficients that represent significant features across scales. Table 2.1 shows the previous study of de-noising.

Table 2.1: Summary of previous study

Images	Algorithms	References
Ultrasound Image	Wavelet Thresholding	[5]
	Novel Bayesian Multiscale	[7]
Magnetic resonance image (MRI)	Nonlinear anisotropic	[10]
	wavelet transforms	[11]
Computed tomography (CT)	multi-dimensional adaptive filter	[14]
	Edge-preserving Adaptive Filters	[15]

2.2 Medical imaging

Medical imaging is the technique and process used to create images of the human body (or parts and function thereof) for clinical purposes (medical procedures seeking to reveal, diagnose or examine disease) or medical science (including the study of normal anatomy and physiology) [16]. Although imaging of removed organs and tissues can be performed for medical reasons, such procedures are not usually referred to as medical imaging. As a discipline and in its widest sense, it is part of biological imaging and incorporates radiology (in the wider sense), nuclear medicine, investigative radiological sciences, endoscopy, (medical) thermography, medical photography and microscopy (e.g. for human pathological investigations). Measurement and recording techniques which are not primarily designed to produce images, such as electroencephalography (EEG), magneto encephalography (MEG), Electrocardiography (EKG) and others, but which produce data susceptible to be represented as maps, can be seen as forms of medical imaging [17].

Radiation exposure from medical imaging in 2006 made up about 50% of total ionizing radiation exposure in the United States. In the clinical context, "invisible light" medical imaging is generally equated to radiology or "clinical imaging" and the medical practitioner responsible for interpreting (and sometimes acquiring) the images is a radiologist. "Visible light" medical imaging involves digital video or still pictures that can be seen without special equipment. Dermatology and wound care are two modalities that utilize visible light imagery. Diagnostic radiography designates the technical aspects of medical imaging and in particular the acquisition of medical images. The radiographer or radiologic technologist is usually responsible for acquiring medical images of diagnostic quality, although some radiological interventions are performed by radiologists. While radiology is an evaluation of anatomy, nuclear medicine provides functional assessment [18]. Many of the techniques developed for medical imaging also have scientific and industrial applications. Medical imaging is often perceived to designate the set of techniques that non-invasively produce images of the internal aspect of the body. In this restricted sense, medical imaging can be seen as the solution of mathematical inverse problems. This means that cause (the properties of living tissue) is inferred from effect (the observed signal). In the case of ultrasonography the probe consists of ultrasonic pressure waves and echoes inside the tissue show the internal structure. In the case of projection radiography, the probe is X-ray radiation which is absorbed at different rates in different tissue types such as bone, muscle and fat. The term noninvasive is a term based on the fact that following medical imaging modalities do not penetrate the skin physically. But on the electromagnetic and radiation level, they are quite invasive. From the high energy photons in X-Ray Computed Tomography, to the 2+ Tesla coils of an MRI device, these modalities alter the physical and chemical environment of the body in order to obtain data [19].

2.3 Comparison between MRI and ultrasound imaging

Digital medical images involving many types of images which are different from one to another in terms of how is produced and how it is look. In this study MRI images and ultrasound images are used and Table 2.2 describes the difference between them.

Table 2.2: Comparison between MRI and Ultrasound

Image	Ultrasound	Magnetic Resonance Image (MRI)
History	**1794**, Lazzaro Spallanzini, Bats navigation Francis Galton Galton whistle (above audible frequency) **1881,** Gabriel Lippman, Reciprocal behavior of achieving a mechanical stress in response to a voltage difference was mathematically deduced. Generation and reception of 'ultrasound' **1942,** Dr. Karl Dussik, transmission ultrasound investigation of the brain Two devices, emitter and receiver.	**1973**, Paul Lauterbur (Zeugmatography). **1975**, Richard Ernst (2D NMR). **1977**, Raymond Damadian (FONAR Corporation). **1984**, FONAR Corporation receives FDA approval for its first MRI scanner. **1986**, Jürgen Hennig, A. Nauerth, and Hartmut Friedburg(RARE). **1988**, Schering's MAGNEVIST gets its first approval by the FDA. **1991**, MRI was developed independently by the University of Minnesota. **1992 – 1997,** Fonar, infringement patents in the MRI industry.
Operation	❖ Place small transducer against the skin. ❖ Emits high frequency sound waves. ❖ Detects bounce back waves. ❖ Different tissues reflect different waves. ❖ Reconstruction software Viewing structure on a screen. 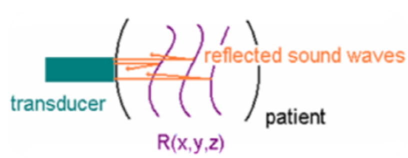	❖ Body :strong magnetic field. ❖ Machine uses :strong magnetic field and pulses of radio waves. ❖ Machine creates an image :how hydrogen atoms react. ❖ Usually images are created as single slices of organs or structures. ❖ MRI computer combine them to give a 3 D image. 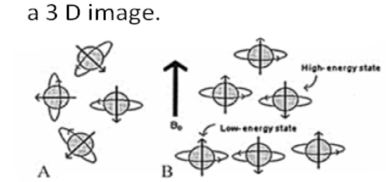
Image Features	• Non-invasive • Inexpensive • No harmful • Suitable for soft tissues • Detect lesions in women • Tell the difference between a cyst and a solid mass • Detect blood flow through vessels. • Can be portable. • Real-time imaging. • Monitoring during treatment.	• No Ionizing Radiation. • MRI can give a three-dimensional depiction of the brain. • Contrast resolution • Obtain direct and oblique image. • Differentiate between acute and chronic transit and fibrous. • No adverse effects. • MRI maps the distribution of water molecules.

2.4 Image noise

Image noise is the random variation of brightness or color information in images produced by the sensor and circuitry of a scanner or digital camera. Image noise can also originate in film grain and in the unavoidable shot noise of an ideal photon detector [20]. Image noise is generally regarded as an undesirable by-product of image capture. Although these unwanted fluctuations became known as "noise" by analogy with unwanted sound they are inaudible and actually beneficial in some applications, such as dithering. The characteristics of noise depend on its source. The filter or the operator which best reduces the effect of noise also depends on the source [21]. Many image-processing packages contain operators to artificially add noise to an image. Deliberately corrupting an image with noise allows us to test the resistance of an image-processing operator to noise and assess the performance of various noise filters.

2.4.1 Amplifier Noise (Gaussian Noise)

The standard model of amplifier noise is additive, Gaussian, independent at each pixel and independent of the signal intensity.In color cameras where more amplification is used in the blue color channel than in the green or red channel, there can be more noise in the blue channel .Amplifier noise is a major part of the "read noise" of an image sensor, that is, of the constant noise level in dark areas of the image [20]. Gaussian noise is statistical noise that has its probability density function equal to that of the normal distribution, which is also known as the Gaussian distribution. In other words, the values that the noise can take on are Gaussian-distributed. A special case is white Gaussian noise, in which the values at any pairs of times are statistically independent (and uncorrelated). In applications, Gaussian noise is most commonly used as additive white noise to yield additive white Gaussian noise. If the white noise sequence is a Gaussian sequence, then is called a white Gaussian noise (WGN) sequence [21].

2.4.2 Salt-and-pepper Noise

An image containing salt-and-pepper noise will have dark pixels in bright regions and bright pixels in dark regions [20]. This type of noise can be caused by dead pixels, analog-to-digital converter errors, bit errors in transmission, etc.This can be eliminated in large part by using dark frame subtraction and by interpolating around dark/bright pixels. This noise is named for the salt and pepper appearance an image takes on after being degraded by this type of noise [21].

2.4.3 Speckle Noise

Speckle noise is a granular noise that inherently exists in and degrades the quality of the active radar and synthetic aperture radar (SAR) images. Speckle noise in conventional radar results from random fluctuations in the return signal from an object that is no bigger than a single image-processing element. It increases the mean grey level of a local area. Speckle noise is caused by signals from elementary scatterers, the gravity-capillary ripples, and manifests as a pedestal image, beneath the image of the sea waves. [22].

2.5 Classification of De-noising filters

As shown in Figure 2.1, there are two basic approaches to image de-noising, spatial filtering methods and transform domain filtering methods [23]. A traditional way to remove noise from image data is to employ spatial filters. Spatial filters can be further classified into non-linear and linear filters. Filtering operations in the wavelet domain can be subdivided into linear and nonlinear methods.

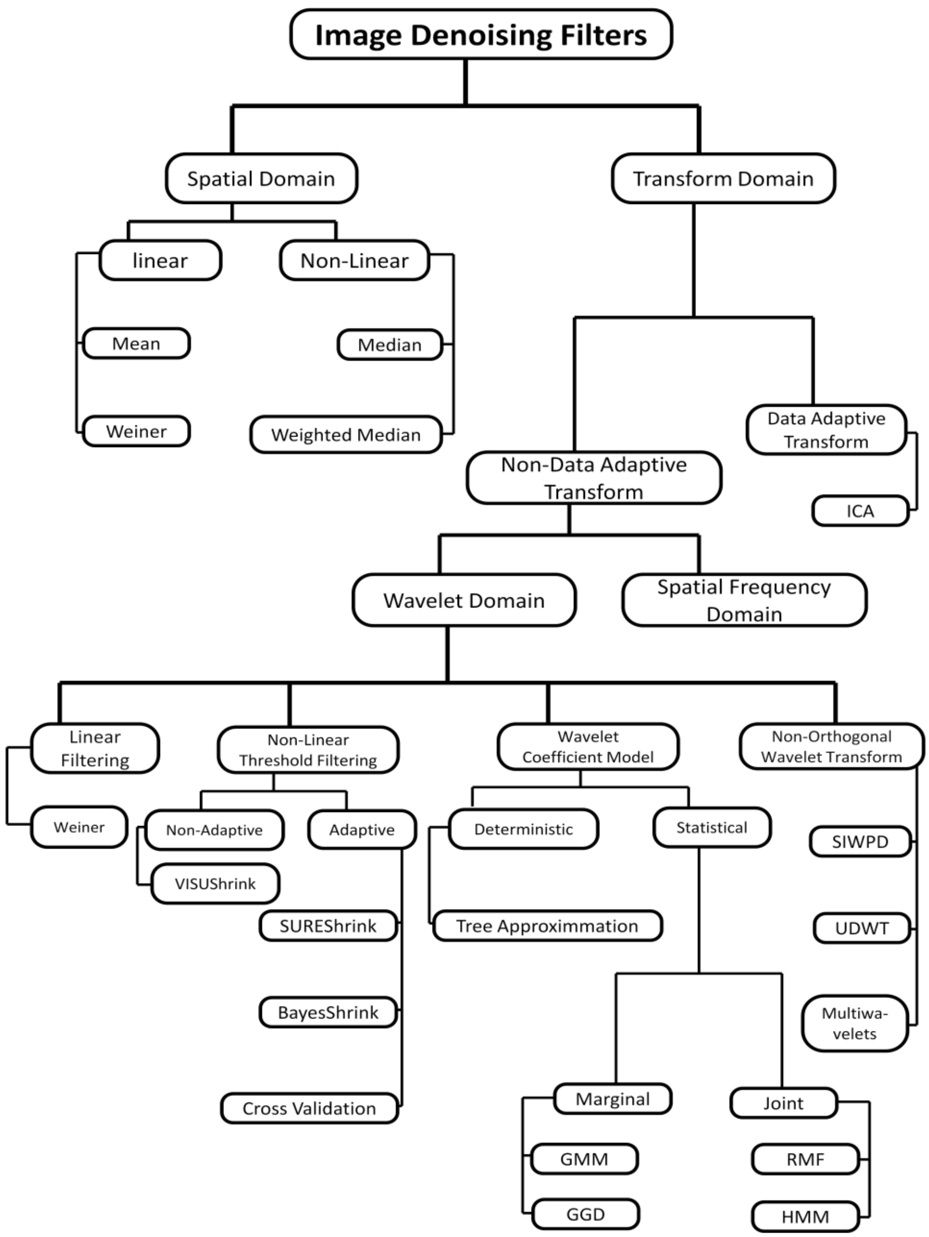

Figure 2.1: Classification of De-noising Algorithms

2.6 De-noising filters review

2.6.1 Median filter

The median filter is a popular nonlinear digital filtering technique, often used to remove noise. Such noise reduction is a typical pre-processing step to improve the results of later processing (for example, edge detection on an image). Median filtering is very widely used in digital image processing because under certain conditions, it preserves edges while removing noise [24]. Sometimes known as a rank filter, this spatial filter suppresses isolated noise by replacing each pixel's intensity by the median of the intensities of the pixels in its neighbourhood. It is widely used in de-noising and image smoothing applications. Median filters exhibit edge-preserving characteristics (cf. linear methods such as average filtering tends to blur edges), which is very desirable for many image processing applications as edges contain important information for segmenting, labelling and preserving detail in images. This filter may be represented by Eq (2).

$$G(u,v) = median\{I\ (x,y),(x,y) \in wF\} \qquad (2)$$

where

$wF\ =\ w\ x\ w$ Filter window with pixel (u,v) as its middle

2.6.2 Gaussian filter

Gaussian filter is a filter whose impulse response is Gaussian function [25]. Gaussian filters are designed to give no overshoot to a step function input while minimizing the rise and fall time. This behaviour is closely connected to the fact that the Gaussian filter has the minimum possible group delay. Mathematically, a Gaussian filter modifies the input signal by convolution with a Gaussian function; this transformation is also known as the Weierstrass transform. Smoothing is commonly undertaken using linear filters such as the Gaussian function (the kernel is based on the normal distribution curve), which tends to produce good results in reducing the influence of noise with respect to the image. The 1D and 2D Gaussian distributions with standard deviation for a data point (*x*) and pixel (*x*,*y*), are given by Eq (3) and Eq (4), respectively [26].

$$G(x) = \frac{1}{2\pi\sigma^2} . e^{-\frac{x^2}{2\sigma^2}} \tag{3}$$

$$G(x,y) = \frac{1}{2\pi\sigma^2} . e^{-\frac{x^2+y^2}{2\sigma^2}} \tag{4}$$

The kernel could be extended to further dimensions as well. For an image, the 2D Gaussian distribution is used to provide a point-spread; i.e. blurring over neighbouring pixels. This is implemented on every pixel in the image using the convolution operation. The degree of blurring is controlled by the sigma or blurring coefficient, as well as the size of the kernel used (squares with an odd number of pixels; e.g. 3×3, 5×5 pixels, so that the pixel being acted upon is in the middle). The processing can be speeded up by implementing the filtering in the frequency rather than spatial domain, especially for the slower convolution operation (which is implemented as the faster multiplication operation in the frequency domain).

2.6.3 Wiener filter

Wiener filters are a class of optimum linear filters which involve linear estimation of a desired signal sequence from another related sequence. It is not an adaptive filter. The wiener filter’s main purpose is to reduce the amount of noise present in a image by comparison with an estimation of the desired noiseless image. The Wiener filter may also be used for smoothing. This filter is the mean squares error-optimal stationary linear filter for images degraded by additive noise and blurring. It is usually applied in the frequency domain (by taking the Fourier transform) [21], due to linear motion or unfocussed optics Wiener filter is the most important technique for removal of blur in images. From a signal processing standpoint. Each pixel in a digital representation of the photograph should represent the intensity of a single stationary point in front of the camera. Unfortunately, if the shutter speed is too slow and the camera is in motion, a given pixel will be an amalgram of intensities from points along the line of the camera's motion.

The goal of the Wiener filter is to filter out noise that has corrupted a signal. It is based on a statistical approach. Typical filters are designed for a desired frequency response. The Wiener filter approaches filtering from a different angle. One is assumed to have knowledge of the spectral properties of the original signal and the noise, and one seeks the LTI filter whose output would come as close to the original signal as possible [27]. Wiener filters are characterized by the following:

1. Assumption: signal and (additive) noise are stationary linear random processes with known spectral characteristics.

2. Requirement: the filter must be physically realizable, i.e. causal (this requirement can be dropped, resulting in a non-causal solution).

3. Performance criteria: minimum mean-square error.

Wiener Filter in the Fourier Domain as in Eq (5).

$$G(u,v) = \frac{H^{*}(u,v)P_{s}(u,v)}{|H\ (u,v)\ |^{2}\ P_{s}(u,v) + P_{n}(u,v)} \tag{5}$$

Where

$H(u,v)$ = Fourier transform of the point spread function

$Ps(u,v)$ = Power spectrum of the signal process, obtained by taking the Fourier transform of the signal autocorrelation

$Pn(u,v)$ = Power spectrum of the noise process, obtained by taking the Fourier transform of the noise autocorrelation

It should be noted that there are some known limitations to Wiener filters. They are able to suppress frequency components that have been degraded by noise but do not reconstruct them. Wiener filters are also unable to undo blurring caused by band limiting of $H(u,v)$, which is a phenomenon in real-world imaging systems.

2.7 Peak Signal-to-Noise Ratio (PSNR)

Peak signal-to-noise ratio (PSNR) is the ratio between a signal's maximum power and the power of the signal's noise. Engineers commonly use the PSNR to measure the quality of reconstructed images that have been compressed. Each picture element (pixel) has a colour value that can change when an image is compressed and then uncompressed. Signals can have a wide dynamic range, so PSNR is usually expressed in decibels, which is a logarithmic scale [28].

The PSNR is most commonly used to measure quality of reconstruction of lossy compression codecs (e.g., for image compression). The signal in this case is the original data, and the noise is the error introduced by compression. When comparing compression codecs it is used as an approximation to human perception of reconstruction quality, therefore in some cases one reconstruction may appear to be closer to the original than another, even though it has a lower PSNR (a higher PSNR would normally indicate that the reconstruction is of higher quality). One has to be extremely careful with the range of validity of this metric; it is only conclusively valid when it is used to compare results from the same codec (or codec type) and same content [29]. It is most easily defined via the mean squared error (*MSE*), where it denotes the mean square error for two $m \times n$ images *I (i, j)& I (i, j)* where one of the images is considered a noisy approximation of the other and is given by Eq (6) and Eq (7).

$$MSE = \frac{1}{mn} \sum_{i=0}^{m-1} \sum_{j=0}^{n-1} [I(i,j) - K(i,j)]^2 \qquad (6)$$

The *PSNR* is defined by Eq (7)

$$\mathrm{PSNR_{dB}} = 10 \cdot \log_{10} \left(\frac{\mathrm{MAX_I^2}}{\mathrm{MSE}} \right) \qquad (7)$$

Where, MAX_I is the maximum possible pixel value of the image. When the pixels are represented using 8 bits per sample, which is equal to 255.

Typical values for the PSNR in lossy image and video compression are between 30 and 50 dB, where higher is better. Acceptable values for wireless transmission quality loss are considered to be about 20 dB to 25 dB [30].

CHAPTER III

METHODOLOGY

3.1 The concept of de-noising filters

The idea of every de-noising filter is different from other filters because every filter has its own function. To give simple explanation of the de-noising filters window 3×3 is used for median, Gaussian and Wiener filter.

Before the beginning of the discretion of de-noising filters we have to understand the convolution.

3.1.1 Convolution

Convolution is a simple mathematical operation which is fundamental for many common image processing operators. Convolution provides a way of `multiplying together' two arrays of numbers, generally of different sizes, but of the same dimensionality, to produce a third array of numbers of the same dimensionality. This can be used in image processing to implement operators whose output pixel values are simple linear combinations of certain input pixel values [31].

In an image processing context, one of the input arrays is normally just a gray level image. The second array is usually much smaller, and is also two-dimensional (although it may be just a single pixel thick), and is known as the kernel. Figure 3.1, shows an example image and kernel that we will use to illustrate convolution.

I1	I2	I3	I4	I5	I6	I7	I8	I9	I10
I11	I12	I13	I14	I15	I16	I17	I18	I19	I20
I21	I22	I23	I24	I25	I26	I27	I28	I29	I30
I41	I42	I43	I44	I45	I46	I47	I48	I49	I50
I51	I52	I53	I54	I55	I56	I57	I58	I59	I60
I61	I62	I63	I64	I65	I66	I67	I68	I69	I70
I71	72	I73	I74	I75	I76	I77	I78	I79	I80
I81	I82	I83	I84	I85	I86	I87	I88	I89	I90
I91	I92	I93	I94	I95	I96	I97	I98	I99	I100

(a)

K11	K12	K13
K21	K22	K23
K31	K32	K33

(b)

Figure 3.1: (a) Pixels of image (b) Kernel of filter

The convolution is performed by sliding the kernel over the image, generally starting at the top left corner, so as to move the kernel through all the positions where the kernel fits entirely within the boundaries of the image. Each kernel position corresponds to a single output pixel, the value of which is calculated by multiplying together the kernel value and the underlying image pixel value for each of the cells in the kernel, and then adding all these numbers together. So, in our example, the value of the bottom right pixel in the output image will be given by Eq (8).

$$O1 = I1\; k11 + I2\; K12 + I3\; K13 + I11\; K21 + I12\; K22 + I13\; KK23 + I21\; K31 + I22\; K32 + I23\; K33 \qquad (8)$$

If the image has M rows and N columns, and the kernel has m rows and n columns, then the size of the output image will have M - m + 1 rows, and N - n + 1 columns. Mathematically we can write the convolution as Eq (9).

$$O(i,j) = \sum_{k=1}^{m}\sum_{l=1}^{n} I(i+k-1, j+l-1)K(k,l) \qquad (9)$$

where i runs from 1 to M - m + 1 and j runs from 1 to N - n + 1.

3.1.2 How does Median filter work?

The median filter considers each pixel in the image in turn and looks at its nearby neighbours to decide whether or not it is representative of its surroundings. Instead of simply replacing the pixel value with the *mean* of neighbouring pixel values, it replaces it with the median of those values [21].

Median filter controls the pepper and Gaussian noises. The median filter is reputed to be edge preserving. The transfer function used here in Eq (10)

$$T\ (x, y) = \ I\left(\frac{(n\ x\ n)}{2}\right) \qquad (10)$$

$$I1 \ \leq \ I2 \ \leq \ I3 \ \leq \ \ldots \ \leq \ In\ x\ n$$

where $I\ (n\ x\ n)\ /\ 2$ is the intensity value in the middle position of the sorted array of the neighbouring pixels.

0	0	0
0	12	9
0	22	17

Neighbourhood values are (0, 0, 0, 0, 0, 4, 4, 12, 22)

Median value is 0

Figure 3.2: Sorting neighbourhood values and determine median value

The median is calculated by first sorting all the pixel values from the surrounding neighbourhood into numerical order and then replacing the pixel being considered with the middle pixel value as was showed in Figure 3.2. If the neighbourhood under consideration contains an even number of pixels, the average of the two middle pixel values is used. The pattern of neighbours is called the "window", which slides, pixel by pixel over the entire image.

12	9	14	13	7	9	4	5	13	4
22	17	11	10	18	7	4	6	9	22
5	2	3	21	2	1	4	2	13	0
13	14	5	13	4	1	2	3	11	5
19	4	17	6	2	6	20	3	2	0
15	9	2	11	4	7	8	11	4	6
8	15	5	11	3	9	7	12	10	4
9	8	17	4	2	9	10	8	15	21
11	4	7	8	15	6	21	3	2	9
10	14	18	7	4	17	10	6	7	3

Figure 3.3: Assumed pixels window represented on MRI image

Median filtering using a 3×3 sampling window with the extending border values outside with 0s

0	0	0	0	0	0	0	0	0	0	0	0
0	12	9	14	13	7	9	4	5	13	4	0
0	22	17	11	10	18	7	4	6	9	22	0
0	5	2	3	21	2	1	4	2	13	0	0
0	13	14	5	13	4	1	2	3	11	5	0
0	19	4	17	6	2	6	20	3	2	0	0
0	15	9	2	11	4	7	8	11	4	6	0
0	8	15	5	11	3	9	7	12	10	4	0
0	9	8	17	4	2	9	10	8	15	21	0
0	11	4	7	8	15	6	21	3	2	9	0
0	10	14	18	7	4	17	10	6	7	3	0
0	0	0	0	0	0	0	0	0	0	0	0

Figure 3.4: Movement of the window 3×3 (mask) on the pixels

0	0	0	0	0	9	12	17	22
0	0	0	9	11	12	14	17	22
0	0	0	9	10	11	13	14	17

Figure 3.5: Sorting the pixels and determining middle pixel value

0	11	10	10	7	4	4	4	5	0
5	11	11	11	9	4	4	5	6	4
5	11	11	10	7	4	3	4	6	5
4	5	6	5	4	2	3	3	3	0
9	13	9	5	6	4	6	4	4	2
8	9	9	5	6	7	8	8	4	2
8	9	9	4	7	7	9	10	10	4
8	8	8	7	8	9	9	10	9	4
8	10	8	7	7	10	9	8	7	3
0	7	7	7	6	6	6	3	3	0

Figure 3.6: Pixels window after applying Median filter on all pixels

3.1.3 How does Gaussian filter work?

Gaussian filter are a class of low-pass filter, all based on the Gaussian probability distribution function used to blur images and remove noise and detail. In one dimension, the Gaussian function is here in Eq (11).

$$G(x) = \frac{1}{2\pi\sigma^2} . e^{-\frac{x^2}{2\sigma^2}} \qquad (11)$$

Where σ is the standard deviation of the distribution The distribution is assumed to have a mean of 0. Shown graphically, we see the familiar bell shaped Gaussian distribution, where a large value of σ produces to a flatter curve, and a small value leads to a "pointier" curve. Figure 3.7 shows examples of such one dimensional Gaussians [25].

Large value of σ Small value of σ

Figure 3.7: One dimensional Gaussians

When working with images, we need to use the two dimensional Gaussian function Figure 3.8. This is simply the product of two 1D Gaussian functions (one for each direction) and is given by Eq (12).

$$G(x,y) = \frac{1}{2\pi\sigma^2} . e^{-\frac{x^2+y^2}{2\sigma^2}} \qquad (12)$$

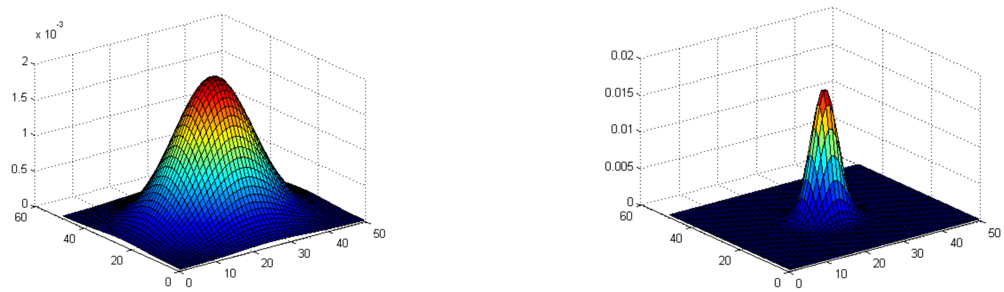

$\sigma = 9$ $\qquad$ $\sigma = 3$

Figure 3.8: Two dimensional Gaussians

The Gaussian filter works by using the 2D distribution as a point-spread function. This is achieved by convolving the 2D Gaussian distribution function with the image. Before we can perform the convolution a collection of discrete pixels we need to produce a discrete approximation to the Gaussian function. In theory, the Gaussian distribution is non-zero everywhere, which would require an infinitely large convolution kernel, but in practice it is effectively zero more than about three standard deviations from the mean, and so we can truncate the kernel at this point. The kernel coefficients diminish with increasing distance from the kernel's centre. Central pixels have a higher weighting than those on the periphery [25]. Larger values of σ produce a wider peak (greater blurring). Kernel size must increase with increasing σ to maintain the Gaussian nature of the filter. Gaussian kernel coefficients depend on the value of σ. Figure 3.9 shows a different convolution kernel that approximates a Gaussian with σ.

0.063	0.125	0.063
0.125	0.250	0.125
0.063	0.125	0.063

0.075	0.124	0.075
0.124	0.204	0.124
0.075	0.124	0.075

0.102	0.115	0.102
0.115	0.131	0.115
0.102	0.115	0.102

Figure 3.9: 3×3 windows with $\boldsymbol{\sigma} = 0.849$, $\boldsymbol{\sigma} = 1$, $\boldsymbol{\sigma} = 2$

The idea of these windows distribution comes from

$$\frac{1}{16} \times \begin{bmatrix} 1 & 2 & 1 \\ 2 & 4 & 2 \\ 1 & 2 & 1 \end{bmatrix} = \begin{bmatrix} 0.063 & 0.125 & 0.063 \\ 0.125 & 0.250 & 0.125 \\ 0.063 & 0.125 & 0.063 \end{bmatrix}$$

Figure 3.10: 3×3 windows with σ = 0.849

Where $\sigma = 0.849$ and 16 is the summation of the values in 3×3 window with $\sigma = 0.849$ this window is using to explain how Gaussian filter is working by convolute it on the pixels of MRI.

12	9	14	13	7	9	4	5	13	4
22	17	11	10	18	7	4	6	9	22
5	2	3	21	2	1	4	2	13	0
13	14	5	13	4	1	2	3	11	5
19	4	17	6	2	6	20	3	2	0
15	9	2	11	4	7	8	11	4	6
8	15	5	11	3	9	7	12	10	4
9	8	17	4	2	9	10	8	15	21
11	4	7	8	15	6	21	3	2	9
10	14	18	7	4	17	10	6	7	3

Figure 3.11: Assumed pixels window represented on MRI image

0	0	0	0	0	0	0	0	0	0	0	0
0	12	9	14	13	7	9	4	5	13	4	0
0	22	17	11	10	18	7	4	6	9	22	0
0	5	2	3	21	2	1	4	2	13	0	0
0	13	14	5	13	4	1	2	3	11	5	0
0	19	4	17	6	2	6	20	3	2	0	0
0	15	9	2	11	4	7	8	11	4	6	0
0	8	15	5	11	3	9	7	12	10	4	0
0	9	8	17	4	2	9	10	8	15	21	0
0	11	4	7	8	15	6	21	3	2	9	0
0	10	14	18	7	4	17	10	6	7	3	0
0	0	0	0	0	0	0	0	0	0	0	0

Figure 3.12: Movement of the window 3 x 3 (mask) on the pixels

To achieve the function of Gaussian filter, the 2D Gaussian distribution of 3×3 window with $\sigma = 0.849$ must be convolved on the first window of MRI pixels to get first value of filtered pixel.

$$\frac{1}{16} \times \begin{bmatrix} 1 & 2 & 1 \\ 2 & 4 & 2 \\ 1 & 2 & 1 \end{bmatrix} \times \begin{bmatrix} 0 & 0 & 0 \\ 0 & 12 & 9 \\ 0 & 22 & 17 \end{bmatrix}$$

Figure 3.13: 3×3 windows with σ = 0.849, first window of MRI pixels

$$1st\ P = \frac{1 \times 0 + 2 \times 0 + 1 \times 0 + 2 \times 0 + 4 \times 12 + 2 \times 9 + 1 \times 0 + 2 \times 22 + 1 \times 17}{16}$$

$$1st\ filtered\ pixel = \frac{1127}{16} = 7.9375 = \boxed{8}$$

[1] S. Arivazhagan, S. Deivalakshmi, K. Kannan, B.N.Gajbhiye, C.Muralidhar, Sijo N Lukose, M.P.Subramanian, “Performance Analysis of Wavelet Filters for Image Denoising”, Advances in Computational Sciences and Technology, Vol.1 No. 1 (2007), pp. 1–10, ISSN 0973-6107.

[2] Nguyen Thanh Binh and Ashish Khare, "Adaptive complex wavelet technique for medical image denoising," in proceedings of the third International Conference on the development of Biomedical Engineering, pp. 195-198, Vietnam, January 11-14, 2010

[3] Y. Wang and H. Zhou, “Total variation wavelet-based medical image de-noising” School of Mathematics, Georgia Institute of Technology, Atlanta, GA 30332-0430, USA, 2006.

[4] B. Goossens, A. Pizurica, and W. Philips. Image denoising using mixtures of projected Gaussian scale mixtures, IEEE Transactions on Image Processing, Vol.18, Issue. 8, pp.1689-1702, 2009.

[5] S. Sudha,., G. Suresh,. and R Sukanesh. Speckle noise reduction in ultrasound images using context-based adaptive wavelet thresholding, IETE journal, Vol. 55, pp 135-143, 2009.

[6] S. Solbø and T. Eltoft, “A Stationary Wavelet-Domain Wiener Filter for Correlated Speckle”, IEEE Transactions on geoscience and remote sensing, vol. 46, NO. 4, APRIL 2008.

[7] A. Achim, and A. Bezerianos. Novel Bayesian Multiscale Method for Speckle Removal in Medical Ultrasound Images, IEEE Transactions on Medical Imaging, Vol. 20, No. 8,pp.772-783, 2001.

[8] P. Perona and J. Malik. Scale-space and edge detection using anisotropic diffusion. IEEE Trans. Pattern Anal. Mach. Intell., 12(7):629–639, July 1990.

[9] M. Lysaker, A. Lundervold, and X. Tai. Noise removal using fourth-order partial differential equation with applications to medical magnetic resonance images in space and time. IEEE Trans. Imag. Proc., 2003.

[10] G. Gerig, O. Kubler, R. Kikinis, and F. A. Jolesz. Nonlinear anisotropic filtering of MRI data. IEEE Tr. Med. Imaging, 11(2):221-232, 1992.

[11] D. Healy and J. Weaver. Two applications of wavelet transforms in magnetic resonance imaging. IEEE Trans. Info. Theory, 38(2):840-860, 1992.

[12] R. Nowak. Wavelet-based rician noise removal for magnetic resonance imaging. IEEE Trans. Image. Proc., 8:1408-1419, 1999.

[13] A. Pizurica, W. Philips, I. Lemahieu, and M. Acheroy. A versatile wavelet domain noise filtration technique for medical imaging. IEEE Trans. Med. Imaging, 22(3):323-331, 2003.

[14] M. Kachelrie, O. Watzke and W. Generalized. multi-dimensional adaptive filtering for conventional and spiral single-slice, and cone-beam CT.American Association of Physicists in Medicine,vol.28, no.4, 475-490, (2001).

[15] M. Okumura, O. Takamasa, and S. Tsukagoshi .New Method of Evaluating Edge-preserving Adaptive Filters for Computed Tomography (CT) : Digital Phantom Method. Jpn J Radiol Technol, vol.62, no.7, 971-978, (2006).

[16] B.N.Raasch, E.W. Carsky, E. J. Lane, J. P.O'Callaghan, and E. R. Heitzman, "Radiographic anatomy of the interlobar fissures: A study of 100 specimens," Amer. J. Roentgenol., vol. 138, pp. 647–554, 1982.

[17] CA Roobottom, G. Mitchell, Morgan-Hughes. "Radiation-reduction strategies in cardiac computed tomographic angiography". Clin Radiol 65 (11): 859–67. doi:10.1016/j.crad.2010.04.021. G (November 2010)

[18] S.M. Larie and S.S. Abukmeil. “Brain abnormality in schizophrenia: a systematic and quantitative review of volumetric magnetic resonance imaging studies”. J. Psych., 172:110–120, 1998.

[19] Q. Long, X.Y. Xu, M.W. Collins, M. Bourne, and T.M. Griffith. “Magnetic resonance image processing and structured grid generation of a human abdominal bifurcation”. Computer Methods and Programs in Biomedicine, 56:249–259, 1998.

[20] S. Zhong, V.Cherkassky,“Image Denoising using Wavelet Thresholding and Model Selection”. IEEE Trans Image Process 2000. International Conference on, Volume: 3, 10-13 Sept. 2000 Pages: 262.

[21] S. Kumar, P. Kumar, M. Gupta and A. K. Nagawat, “Performance Comparison of Median and Wiener Filter in Image De-noising,” International Journal of Computer Applications 12(4):27–31, December 2010.

[22] S. Kent, O. N. Oçan, and T. Ensari. "Speckle Reduction of Synthetic Aperture Radar Images Using Wavelet Filtering". in ITG, VDE, FGAN, DLR, EADS, astrium. EUSAR 2004 Proceedings, 5th European Conference on Synthetic Aperture Radar, May 25–27, 2004, Ulm, Germany.

[23] M. C. Motwani, M. C. Gadiya, R. C. Motwani and F. C. Harris. “Survey of Image Denoising Techniques”. University of Nevada, Reno Dept of Comp. Sci. & Engr., Reno, NV 89557 USA (775) 784-6571.

[24] H. Raymond Chan, Chung-Wa Ho, and M. Nikolova, "Salt-and-Pepper noise removal by median-type noise detectors and detail-preserving regularization". IEEE Trans Image Process 2005; 14: 1479-1485.

[25] P. Hsiao1, S. Chou, and F. Huang, "Generic 2-D Gaussian Smoothing Filter for Noisy Image Processing". National University of Kaohsiung, Kaohsiung, Taiwan, 2007.

[26] R. Fisher, S. Perkins, A. Walker, E. Wolfart. Gaussian smoothing, Hypermedia image processing reference (HIPR2), 2003. Available from:URL:http:// homepages .inf. ed.ac.uk / rbf/ HIPR2/gsmooth.htm.

[27] Kazubek, "Wavelet domain image de-noising by thresholding and Wiener filtering". M. Signal Processing Letters IEEE, Volume: 10, Issue: 11, Nov. 2003 265 Vol.3.

[28] M. Kachelrie, O. Watzke and W. Generalized. multi-dimensional adaptive filtering for conventional and spiral single-slice, and cone-beam CT.American Association of Physicists in Medicine,vol.28, no.4, 475-490, (2001).

[29] Q. Huynh-Thu and M. Ghanbari, "Scope of validity of PSNR in image/video quality assessment". Electronics Letters 44 (13): 800–801, 2008.

[30] N. Thomos, V. Boulgouris, M. G. Strintzis, "Optimized Transmission of JPEG2000 Streams Over Wireless Channels". IEEE Transactions on Image Processing , 15 (1)2006.

[31] R Fisher, S Perkins, A Walker, E Wolfart. Convolution, Hypermedia image processing reference (HIPR2), 2003. Available from:URL:http:// homepages .inf. ed.ac.uk / rbf/ HIPR2/convolution.htm.

[32] H. Yoshino, C. Dong, Y. Washizawa and Y. Yamashita. "Kernel Wiener Filter and its Application to Pattern Recognition", IEEE Transactions on neural networks, 2010.

[33] T. Wiegand, H. Schwarz, A. Joch, F. Kossentini, and G. Sullivan, "Rate-constrained coder control and comparison of video coding standards", IEEE Trans. Circuits Syst. Video Technol., 2003, 13, (7), pp. 688–703